ISSN 1392 - 1207. MECHANIKA. 2013 Volume 19(2): 178-183

Studying effects of injected flow on drag coefficients over semi perforated circular cylinder

M. Farzaneh-Gord*, A. Molavi**
**Faculty of Mechanical Eng., Shahrood University of Technology, Shahrood, Iran, E-mail: mahmood.farzaneh@yahoo.co.uk*
***Faculty of Mechanical Eng., Shahrood University of Technology, Shahrood, Iran*

crossref http://dx.doi.org/10.5755/j01.mech.19.2.4147

Nomenclature

A - control volume cross section, m^2; A_s - area reference, m^2; C_w - non-dimensional mass flow rate; C_D - drag coefficient; F_D - drag force, N; F_x - force in x direction, N; D - tube diameter, m; L - prototype length, m; m - injected mass flow rate, kg/s; Re - main flow Reynolds number; u - velocity in x direction, m/s; V - air velocity passed through the holes, m/s; V_x - air velocity passed through the holes in x direction, m/s; ν - kinematics viscosity, m^2/s; ρ - density, kg/m^3; μ - dynamic viscosity; Pa×s; $\forall$ - volume, m^3; β - angle of hole's begin, Rad.

Subscript

∞ - free stream condition.

1. Introduction

The secondary flow forced into primary flow through wall holes (injection flow) has numerous uses in industry as an example film cooling. Usually, earlier-stage of nozzle guide vane and gas turbine blades are under the influence of very hot approaching primary flow (hot gases from combustion chamber) with a temperature which is considerably higher than the melting point of the any metals. One way of safeguarding gas turbine blades is to redirect a portion of compressor air and pass it through the nozzles and turbine blades. This cool air (comparing to primary hot gases) forced out from holes within the nozzles and blade makes a layer of cool air around the nozzles and blades (Fig. 1). The gas turbine manufacturers are curious to know both pressure losses and heat exchange in this area.

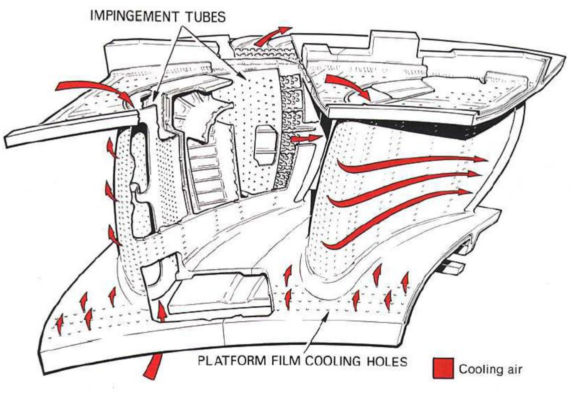

Fig. 1 Cross section of a turbine nozzle guide vane showing film cooling

Flow injection to primary flow is also a method of managing boundary layer flow features. Usually, flow injection makes the boundary layer thicker and reduces surface skin frictions. Recently, there have been substantial interests in the subject of flow injection through surface holes into primary flow theoretically, experimentally and numerically. Simpson [1] conducted a review on previous studies on turbulent boundary layers without and with normal transpiration and expanded the wall law of the wake formulation. Schetz and Nerney [2] have investigated the turbulent boundary layer with perpendicular flow injection and surface roughness by experimental techniques. They prove that turbulence intensity and velocity in the turbulent boundary layer rises as injection flow rate increases. In an experimental work, Yang et al. [3] have studied the influence of uniform perpendicular flow injection into the separated-reattaching flow around a backstep. Bellettre et al. [4] studied a turbulent boundary layer exposed to flow injection through holes in a plate numerically and compared numerical the results with measured values. Kudriavtsev et al. [5] studied the external flow over a flat holed plate with injected cross flow numerically. They reported a significant drag reduction at the interface between the solid surface and the boundary layer and Hwang and Lin [6] forecast thermal and flow fields in a stream with flow injection by utilizing an enhanced low Reynolds number k–epsilon model and direct numerical simulation.

A few numbers of studies on the influences of flow injection through a bluff body on the flow parameters have been carried out. Sucking or blowing flow through two rows of small holes on the cylinder wall has been studied experimentally by Williams et al. [7]. They realized that the generated disturbances considerably changed the frequencies of vortex shedding and pattern of the primary flow. Mathelin et al. [8] have investigated flow injection through the entire surface of a porous circular cylinder numerically. It was realized that the injection tends to raise the boundary layer thickness, to postpone its separation and to reduce the viscous drag produced. Correspondingly, the convective heat transfer is decreased, and in the case of a non-isothermal injection, the surface is very productively defended from the hot free stream flow. The pressure defect at the rear of the circular cylinder tends to “fill up” with blowing, leading to lower transverse static pressure gradients in the near wake.

An experimental investigation on the influence of uniform injection through one holed surface of a square duct on the drag coefficient and pressure distribution has been carried out by Cuhadaroglu et al. [9] in a wind tunnel. The surface pressure distribution around square duct has been measured at three different Reynolds numbers. The effects of injection flow rate, holed surface orientation (i.e., front, top, and rear) on drag coefficient and pressure coefficient are studied. The results reveal that holed surface orientation has strong effects on drag coefficient and pressure coefficient.

In a study carried out by Dong et al. [10], effects of combined leeward blowing and windward suction on flow around a circular cylinder have been studied. Three-dimensional CFD and stability analysis were utilized to quantify the findings for the flow over flexibly mounted and fixed circular cylinders. It is found that small amounts of combined suction and blowing modify the wake instability and resulted to suppression of the fluctuating lift force.

Farzaneh-Gord and Molavi [11] have studied the effects of primary flow Reynolds number, injection flow rate, and the orientation (top, rear and front) of injected flow on pressure distribution over the holed circular cylinder experimentally. They measured pressure around the cylinder using mounted pressure taps. The aim of the current study is to investigate the effects of similar parameters on velocity profile behind the cylinder. Further, the drag coefficient has been calculated based on these velocity profiles and effects of the injected flow are studied. To achieve these goals, a half holed circular cylinder has been studied in low speed wind tunnel experimentally.

2. Experimental apparatus

The experimental investigation has been carried out in Shahrood University of Technology (SUT) low speed wind tunnel. The tunnel is an open circuit type. The test section of the wind tunnel is made of plexiglas which resulted full visibility.

The test section is manufactured in a square shape with 80 cm high, 80 cm wide and 200 cm long. The test section could support various models from sidewalls. The measurements show that the longitudinal freestream turbulence intensity is less than 2% at the lowest air speed (5 m/s) and 0.5% at highest air speed (30 m/s). Over air speed range, and the non-uniformity in velocity at the central portion of the test section is less than 0.5%. Fig. 2 presents the SUT wind tunnel and circular cylinder under investigation.

The free air conditions are measured using a Pitot-static probe, a temperature and a hot wire sensor. From this finding, the air density, viscosity, and velocity are calculated.

The circular cylinder under investigation has dimensions as 80 cm long and 43 mm in diameter. The test object as installed spans the full wind tunnel test section as illustrated in Fig. 2. The test cylinder is made of a steel tube in which a series of 2 mm in diameters holes are bored in middle of the cylinder. Totally, 20 cm of axial length and half of the perimeter of the test object are holed as shown in Fig. 3. The holes are 30 degree apart in circumferential and 3 mm apart in axial direction**.**

Fig. 4 shows all test setup and measured devices. An air compressor has been utilized to provide air supply. The air mass flow rate is managed by a regulating valve and measured by a flow meter.

The data from all sensors are acquired with a data acquisition card (a PCI-6031E 16-bit high-speed board) which installed in a Pentium 4 computer (2-GHz Intel Pentium 4 processor). The signals from the all measuring devices are digitally sampled for a period of 20 s at a rate of 500 Hz.

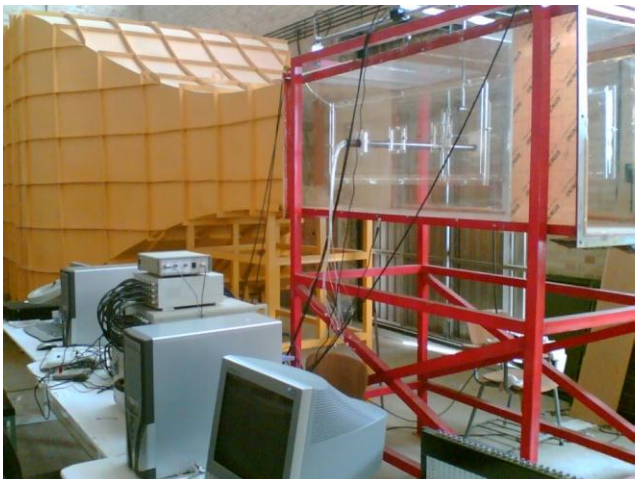

Fig. 2 Shahrood university low speed wind tunnel with installed test cylinder

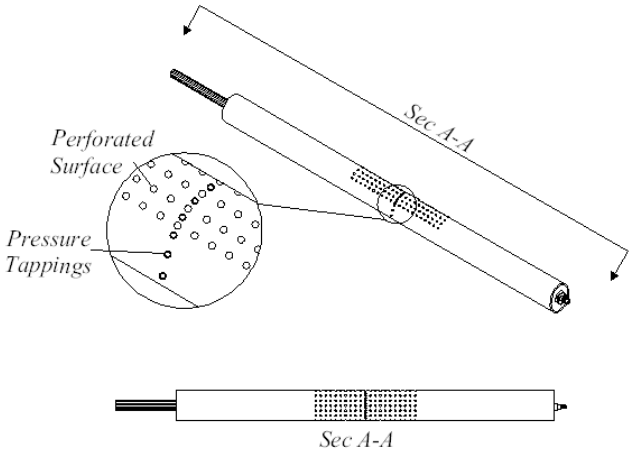

Fig. 3 A schematic diagram of perforated surface circular cylinder

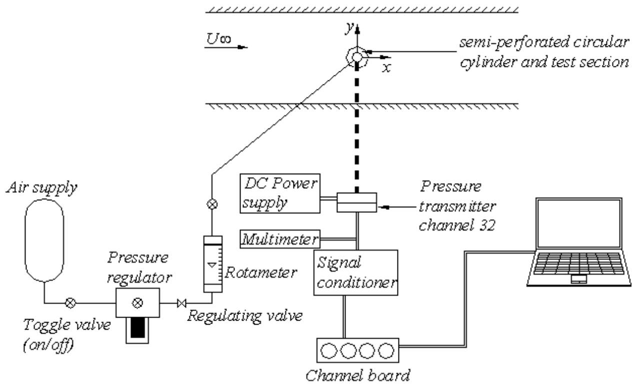

Fig. 4 A schematic diagram of the experimental apparatus and measuring devices

The velocity profile downstream of the test object is measured with the hot wire sensor which sits on a transversing mechanism. This allows the location of the hot wire to be adjusted perpendicular to the free stream flow. A micrometre on the mechanism allows for accurate position measurements.

3. Determining the drag coefficient from velocity profile

The drag force of any object could be calculated from the momentum deficit determined from velocity profile in a wind tunnel. The momentum deficit is calculated from change in velocity profiles in upstream and downstream of the cylinder as illustrated in Fig. 5. The deficit could be considered as momentum lost from the free stream. Integrating velocity profile change at the wake behind the object could give a value for the total drag force acting on the object.

For calculating drag force, velocity profiles should be taken first with the cylinder removed and then with the cylinder positioned at two streamwise locations. This allows calculation of the drag from two different velocity profiles and averaging of the results. The Fluid Mechanics texts [12, 13] are utilized to calculate the drag force on the cylinder from the velocity profiles. The drag force (D) is determined by applying the momentum conservation in a control volume surrounding the cylinder as shown in Fig. 5.

$$\sum F_x = \frac{\partial}{\partial t}\int_{C.V} \rho V d\forall + \int_{C.S} \rho V_x V dA . \quad (1)$$

The first term in RHS is zero and the second term could be expressed as below:

$$\int_{C.S} \rho V_x V dA = -\int_1 \rho U_\infty^2 dA + \int_2 \rho u^2 dA + \int_3 \rho V_x V dA , \quad (2)$$

where $dA = rd\theta$, $V_x = -V\cos\theta$, θ is angle measured the front stagnation point of the cylinder as shown in Fig. 6.

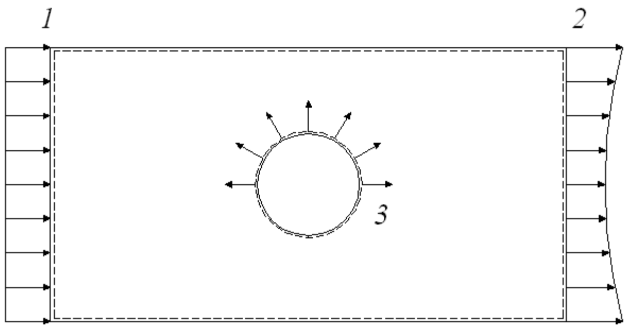

Fig. 5 Control volume enclosing the cylinder

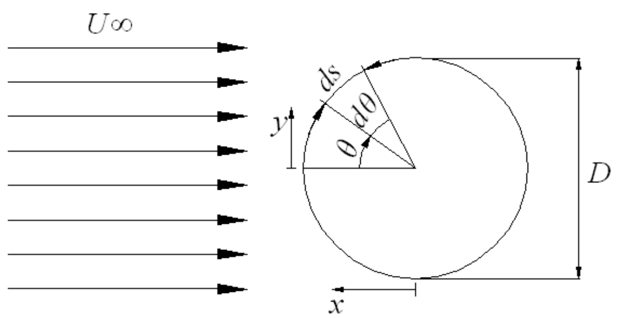

Fig. 6 A schematic diagram of the cylinder with symbols

The Eq. 2, then could be integrated for 3 surfaces as below:

$$\int_{C.S} \rho V_x V dA = \rho\int\left(u^2 - U_\infty^2\right)dA - \int_\beta^{\beta+\pi} V\cos\theta V r d\theta . \quad (3)$$

Considering the Eqs. 3 and 1, one could calculate Drag force as below:

$$F_D = \rho\int\left(u^2 - U_\infty^2\right)dA + \rho D V^2 \sin\beta , \quad (4)$$

where $V = \dfrac{\dot m}{\rho\pi r L}$.

Of particular interest is the Drag coefficient given by the following equation:

$$C_D = \frac{F_D}{\frac{1}{2}\rho U_\infty^2 A_s} = \frac{\int_{-3D}^{3D}\int\left(u^2 - U_\infty^2\right)dA + DV^2\sin\beta}{\frac{1}{2}U_\infty^2 D} , \quad (5)$$

where $A_s = D$.

Non-dimensional parameter effecting the pressure distribution.

Apart from the Reynolds number, *Re*, which is main non-dimensional parameter, the non-dimensional inject flow rate, C_w, will also influence characteristic of flow around the studied cylinder. In this work, the non-dimensional inject flow rate as below has been introduced to investigate the influence of flow rate on drag coefficient:

$$Re = \frac{U_\infty D}{\nu} ; \quad (6)$$

$$C_w = \frac{\dot m}{\mu D} , \quad (7)$$

where $\dot m$ is injected mass flow rate.

4. Results and discussion

The drag coefficient is determined based on Eq. 5 with assisting measured values.

The variation of velocity against height are presented in Fig. 7, 8 and 8 for $Re = 22600$ and $C_w = 1725$. Fig. 7 shows the velocity profiles for the cylinder where the injected flow is opposite of the main flow. As Reynolds numbers increases, the curve height raises due to the increase in the free stream velocity. Higher Reynolds numbers also illustrate a steeper curve. In other way, velocity deficit in the wake regime results to a larger value of drag.

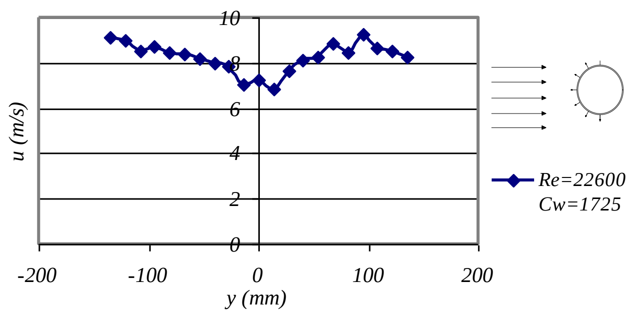

Fig. 7 The velocity profile in wake of the cylinder where injectet flow is opposite to main flow

Fig. 8 shows the velocity profiles for the cylinder where the injected flow is upright of the main flow. It could be realized that the center of the wake remains in the center of the tunnel (the wake remains symmetric).

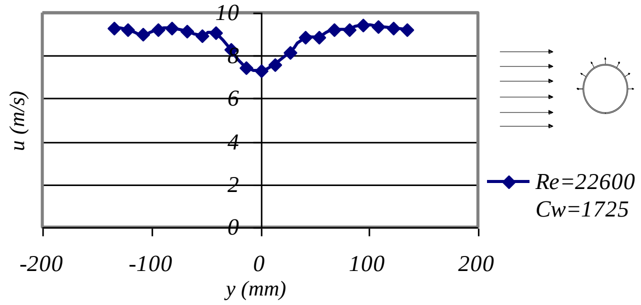

Fig. 8 The velocity profile in wake of the cylinder where injectet flow is upright

The symmetrically of the wake could be also found in the case where the injectet flow is parallel to main flow in Fig. 9.

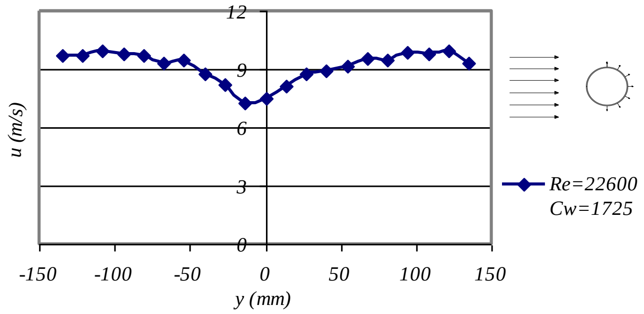

Fig. 9 The velocity profile in wake of the cylinder where injectet flow is parallel to main flow

The variation of the drag coefficient against Reynolds is depicted in Fig. 10 where injected flow is opposite to the main flow. In the figure, the effect of varying C_w could be also studied. It could be realized for low *Re* number flow, the injected flow has reduced the drag coefficient considerably when compared with a cylinder without injection. As mentioned in [12] and [13-14], for $10000 < Re < 200000$, the drag coefficient for a cylinder without injection is about 1.1. As It could be seen in Fig. 10, as *Re* increases the drag coefficient for all C_w cases approaches 1.1. This suggested that for low Reynolds flow, injected flow could reduce the drag coefficient. Generally, for low Reynolds number flow, the drag coefficient is lower for the case where C_w higher and vise versa.

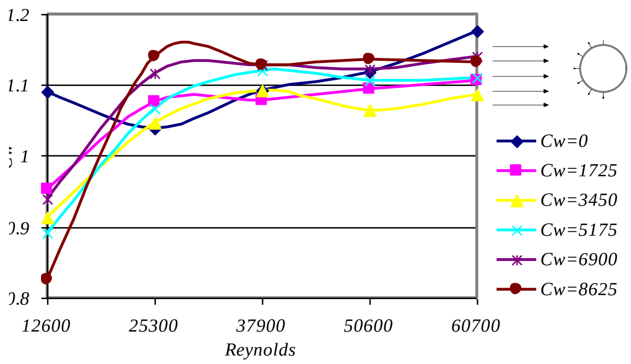

Fig. 10 Variation of pressure drag coefficient where inject flow is opposite to main flow

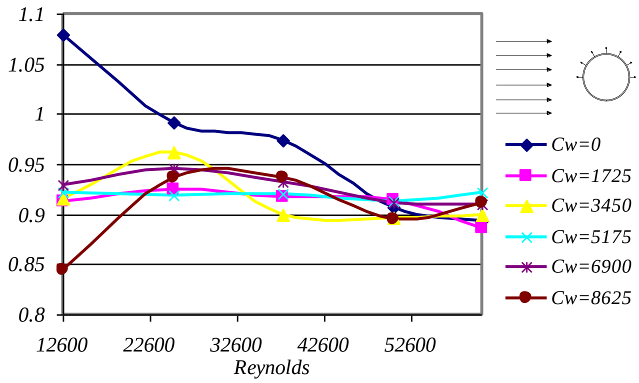

Fig. 11 Variation of pressure drag coefficient where inject flow is upright to main flow

Fig. 11 shows the variation of drag coefficient against Reynolds where injected flow is upright to main flow. In the figure, the effect of varying C_w could be also studied. It could be realized for lowest *Re* number flow, the drag coefficient is lowest for the case where the injected flow is highest. Generally as *Re* increases, the drag coefficient decreases smoothly. For all cases the drag coefficient is lower than 1.1, the drag coefficient for a cylinder without injection.

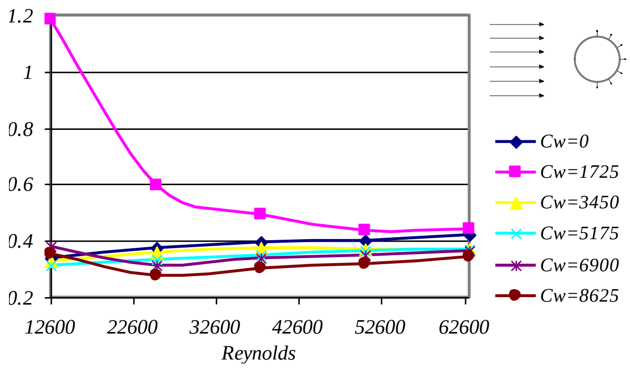

Fig. 12 Variation of pressure drag coefficient where inject flow is parallel to main flow

Fig. 12 shows the variation of the drag coefficient against Reynolds where flow is injected in rear of the cylinder. In the figure, the effect of varying C_w could be also studied. It could be realized for the case where $C_w = 1725$, lowest injected flow rate, the drag coefficient is highest for the case where the injected flow is lowest and as *Re* increases, the drag coefficient decreases sharply. Mainly the drag coefficient is much lower than 1.1, the drag coefficient for a cylinder without injection which suggests a way of reducing the drag coefficient. The low value for drag coefficient is due to the negative pressure at the front of the cylinder.

5. Conclusion

The secondary flow forced into primary flow through wall holes (injection flow) has numerous uses in industry as an example film cooling. Injection flow is also a way of controlling characteristic of boundary layer flow.

In this work, the effects of injection flow rate, the main flow Reynolds number and the direction (front, top or rear) of injected flow on wake behind a half holed circular cylinder has been examined experimentally. The finding shows that, the flow injection affects characteristic of the flow around the circular cylinder.

Based on measured velocity profiles, the drag coefficient has been calculated and presented. The finding also show that flow injection changes the drag coefficient around the cylinder significantly especially for the case, where the flow is injected at the rear of the cylinder. The drag coefficient values show a drop in value for the case where the flow is injected in rear of the cylinder if compared with the drag coefficient for a cylinder without injection. For the case where the flow injects through top of the cylinder, generally the drag coefficient is still lower than the drag coefficient for a cylinder without injection. The results also suggests that for the case where the flow is injected at the front of the cylinder, the drag coefficient could be lower than the drag coefficient for a cylinder without injection for some combination value of the injected flow rate and the main flow Reynolds number.

These suggest that, for the gas turbine blade film cooling, by carefully selecting injected flow rate, the cooling could be achieved while the pressure drop is lowered.

Acknowledgments

This work was supported by research grant from Shahrood University of Technology.

References

1. **Simpson, R.L.** 1970. Characteristics of turbulent boundary layers at low Reynolds numbers with and without transpiration, Journal of Fluid Mechanics 42: 769-802. http://dx.doi.org/10.1017/S002211207000160X.
2. **Schetz, J.A.; Nerney, B.** 1977. Turbulent boundary layer with injection and surface roughness, AIAA Journal 15: 1288-1293. http://dx.doi.org/10.2514/3.7415.
3. **Yang, J.T.; Tsai, B.B.; Tsai, G.L.** 1994. Separated-reattaching flow over a back step with uniform normal mass bleed, ASME Journal of Fluids Engineering 116: 29-35. http://dx.doi.org/10.1115/1.2910236.
4. **Bellettre, J.; Bataille, F; Lallemand, A.** 1999. A new approach for the study of turbulent boundary layers with blowing, International Journal of Heat and Mass Transfer 42: 2905-2920. http://dx.doi.org/10.1016/S0017-9310(98)00341-X.
5. **Kudriavtsev, V.; Braun, M.J.; Hendricks, R.C.** 2001. Virtual experiments on drag reduction, in: Proceedings of the CASI, Toronto, 1-6.
6. **Hwang, C.B.; Lin, C.A.** 2000. Low Reynolds number k–e modeling of flows with transpiration, International Journal for Numerical Methods in Fluids 32: 495-514. http://dx.doi.org/10.1002/(SICI)1097-0363(20000315)32:5<495::AID-FLD920>3.0.CO;2-Q.
7. **Williams C. R.; Mansy H.; Amato C.** 1992. The response of asymmetry properties of a cylinder wake subjected to localized surface excitation, J Fluid Mech, 234: 71-96. http://dx.doi.org/10.1017/S0022112092000703.
8. **Mathelin, L.; Bataille, F.; Lallemand, A.** 2002. The effect of uniform blowing on the flow past a circular cylinder, ASME Journal of Fluids Engineering 124: 452-464. http://dx.doi.org/10.1115/1.1467919.
9. **Cuhadaroglu, B.; Akansu, Y.E.; Turhal, A.O.** 2007. An experimental study on the effects of uniform injection through one perforated surface of a square cylinder on some aerodynamic parameters, Experimental Thermal and Fluid Science 31: 909-915. http://dx.doi.org/10.1016/j.expthermflusci.2006.09.006.
10. **Dong, S.; Triantafyllou, G.S.; Karniadakis, G.E.** 2008. Elimination of vortex streets in bluff-body flows, Physical Review Letters, 100: 204501. http://dx.doi.org/10.1103/PhysRevLett.100.204501.
11. **Farzaneh-Gord, M.; Molavi, A.** 2010. Experimental study of Pressure distribution over semi perforated circular cylinder subjected to injected flow, International Conference on Mechanical and Electrical Technology (ICMET 2010). http://dx.doi.org/10.1109/ICMET.2010.5598476.
12. **White, F.M.** 1999. Fluid Mechanics, McGraw-Hill, New York.
13. **Schlichting, H.; Gersten, K.** 2000. Boundary Layer Theory, 8th edition.
14. **Yahiaoui, T., Adjlout, L., Imine, O.** 2010. Experimental investigation of in-line tube bundles, Mechanika 5(85): 37-43.

M. Farzaneh-Gord, A. Molavi

PER PUSIAU PERFORUOTĄ APSKRITIMINĮ CILINDRĄ ĮPURŠKIAMOS SROVĖS EFEKTO TRAUKOS KOEFICIENTUI NAGRINĖJIMAS

R e z i u m ė

Vidaus pagrindinės srovės įpurškimas per perforuotą paviršių turi daug pramoninių pritaikymų, tokių kaip aušinimo plėvelė. Įpurškimo srovė taip pat naudojama ribinio sluoksnio tekėjimo charakteristikų kontrolei. Šiame darbe atliekamas eksperimentinis tyrimas, nagrinėjantis įpurškimo srovės greičio, pagrindinės srovės, Reynoldso skaičiaus ir įpurškiamos srovės krypties (priekis, viršus, užpakalis) įtaką į greičio profilį už pusiau perforuoto apskritiminio cilindro paviršiaus. Remiantis išmatuotu greičio profiliu, slėgio trauka yra apskaičiuota ir pristatyta. Rezultatai parodė, kad įpurškimo srovė įtakoja tekėjimo per cilindrą ir keičia greičio profilį už cilindro. Lyginant su cilindru be įpurškimo traukos koeficiento dydis mažėja, kai srovė yra įpurškiama cilindro užpakalyje. Tuo atveju, kai srovė yra įpurškiama per cilindro viršų pagrindinis traukos koeficientas yra žemesnis ir tada kai srovė yra įpurškiama cilindro priešakyje traukos koeficientas sumažės kai kurioms srovės įpurškimo greičio ir pagrindinės srovės Reynoldso skaičiaus kombinacijoms.

M. Farzaneh-Gord, A. Molavi

STUDYING EFFECTS OF INJECTED FLOW ON DRAG COEFFICIENTS OVER SEMI PERFORATED CIRCULAR CYLINDER

S u m m a r y

The secondary flow forced into primary flow through wall holes (injection flow) has numerous uses in industry as an example film cooling. Injection flow is also a way of controlling characteristic of boundary layer flow. In this work, an experimental study has been pereformed to investigate the influence of injection flow rate, the main flow Reynolds number and the orientation (front, top or rear) of injected flow on velocity profile behind a half holed circular cylinder. Based on measured velocity profile, the drag coefficient has been calculated and presented. The results show that, the injected flow affects characteristic of the flow over the cylinder and change the velocity profile behind the cylinder. Comparing with a cylinder without injection, the drag coefficient values show a drop in value for the case where the flow is injected in rear of the cylinder. For the case where the flow injects through top of the cylinder, generally the drag coefficient is still lower and for the case where the flow is injected at the front of the cylinder, the drag coefficient could be lowered for some combination value of the injected flow rate and the main flow Reynolds number.

Keywords: Flow over circular cylinder, drag coefficient, flow injection, film cooling.

Received April 15, 2011
Accepted February 11, 2013